

An interactive visualisation for all 2×2 real matrices, with applications to conveying the dynamics of iterative eigenvalue algorithms

Ran Gutin (rg120@ic.ac.uk, Imperial College London)

7th November 2022

Abstract

We present two interactive visualisations of 2×2 real matrices, which we call $v1$ and $v2$. $v1$ is only valid for PSD matrices, and uses the spectral theorem in a trivial way – we use it as a warm-up. By contrast, $v2$ is valid for *all* 2×2 real matrices, and is based on the lesser known theory of Lie Sphere Geometry. We show that the dynamics of iterative eigenvalue algorithms can be illustrated using both. $v2$ has the advantage that it simultaneously depicts many properties of a matrix, all of which are relevant to the study of eigenvalue algorithms. Examples of the properties of a matrix that $v2$ can depict are its Jordan Normal Form and orthogonal similarity class, as well as whether it is triangular, symmetric or orthogonal. Despite its richness, using $v2$ interactively seems rather intuitive.

1 Introduction

We introduce two visualisations in this paper for use in self-study or teaching. We call them $v1$ and $v2$. They are both very simple geometrically. They are as follows:

- $v1$ is perhaps obvious to those well-versed in linear algebra. We treat it as a warm-up. It is valid only for PSD matrices. A matrix is portrayed as an ellipse centred at the origin of \mathbb{R}^2 . This method is an easy consequence of the spectral theorem.
- $v2$ is less obvious to those who know linear algebra because it uses machinery from Lie Sphere Geometry. It is valid *for all* 2×2 real matrices. In “half of cases”, a matrix is portrayed as an unordered pair, consisting of an *oriented circle*, and its *orientation-reversed inversion* through the unit circle.

$v2$ has the advantage that many properties of an arbitrary 2×2 matrix M can quickly be inferred from it:

- Its Jordan Normal Form.
- Which matrices it's orthogonally similar to.
- Its condition number.
- Whether it's upper triangular, lower triangular, diagonal, symmetric, or orthogonal.
- A geometric construction for matrix-vector multiplication: Mv .
- A geometric construction for matrix-matrix multiplication: MK .

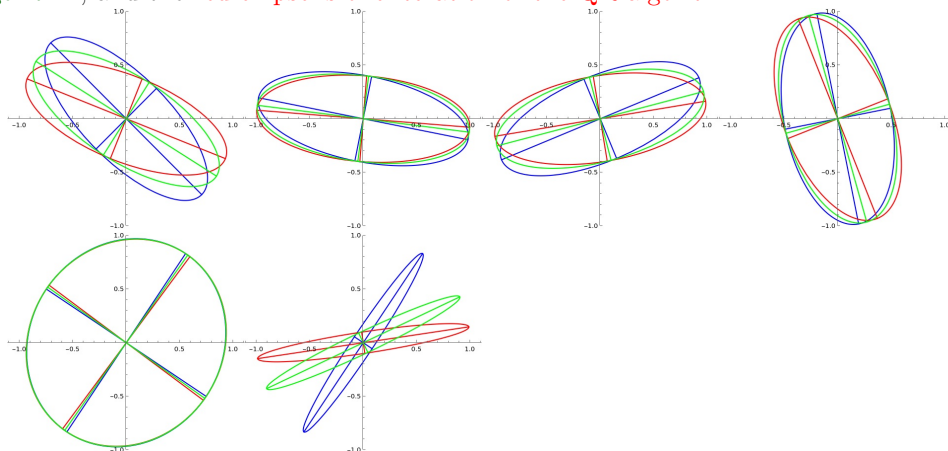
While there are some ways to extend v1 to cover all 2×2 real matrices (for instance by depicting the polar decomposition of M), we don't find that most of the above properties hold. A visualisation that depicts the polar decomposition might still be useful for depicting the dynamics of SVD-finding or polar decomposition-finding algorithms. We don't consider those here as they're rather obvious.

Our approach aims to convey the dynamics of the *unshifted* QR algorithm, without using formulas or theory. Prior pedagogical approaches to the QR algorithm have been considered before in the literature [5, 3], but these are more formula-driven and less visual than ours. Extensions of v2 to 3×3 matrices are formally possible, but raise some issues which are not investigated here.

2 Visualisation v1 (as a warm-up)

The visualisation is **valid only for PSD symmetric matrices**. A 2×2 PSD matrix M is visualised by $\{Mv : v \in \mathbb{R}^2, \|v\|_2 = 1\}$. The visualisation of M is thus always an ellipse, thanks to the spectral theorem.

The **blue ellipse is the input**, the **green ellipse is one iteration of the LR algorithm**, and the **red ellipse is one iteration of the QR algorithm**.



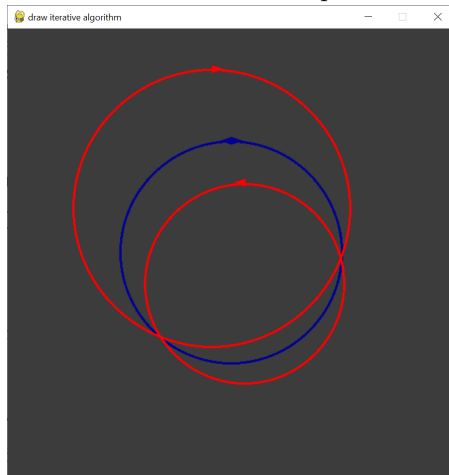
The important points are:

- Convergence happens in every case, though not necessarily quickly.
- Ellipses where the major semi-axis is parallel to the x -axis are attractive fixed points. Convergence near here is fast.
- Ellipses where the major semi-axis is parallel to the y -axis are repulsive fixed points. Convergence near here is slow.
- When the eigenvalues are close to each other, convergence is slow. The ellipses look nearly like circles.
- When one eigenvalue is close to zero, and the other is not, then convergence is fast. The ellipses then look squeezed. They look “opposite to circles”. *Shifting* (at least in the PSD case) can be seen as squeezing an ellipse.

3 Visualisation v2

3.1 Oriented cycles, informally

An example of an *oriented cycle* (note: not necessarily a *circle*) and its *orientation-reversed inversion* is given below. The pair of oriented cycles is in red. There is also a faint dark-blue circle, which represents the unit circle. (Note that we have superimposed two unit circles: One for each possible orientation).



To explain the terminology: A *cycle* is either a point, a circle, or a line. An *oriented cycle* is either:

- a point p , which may be ∞ ,
- an *oriented non-point circle*, which is a pair (B, B^*) , where B is a disk, and B^* is the set of points either inside or outside of B ,
- an *oriented line*, which is a half-plane H . The underlying line is given by the boundary of H .

For each non-point cycle, there are at most two orientations. The orientation can be depicted by drawing an arrow head.

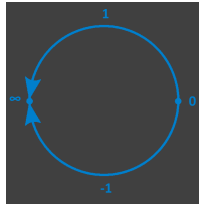
An *inversion* through the unit circle (which is depicted in dark blue) is effectively the map $z \mapsto 1/\bar{z}$ over the complex plane. If one thinks of an oriented cycle C as a point moving in the complex plane (with the orientation being the direction of motion, ignoring both the exact position and speed of the moving point) then the *inversion of C* is given by applying the inversion to the moving point.

An *orientation-reversed inversion* is a transformation which performs an inversion, and then reverses all orientations. The order in which these two operations are performed does not matter.

We denote the orientation-reversed inversion of an oriented cycle C by $\text{ORI}(C)$,

3.2 Projective real line as a circle

The *projective real line* \mathbb{RP}^1 is the set $\mathbb{R} \cup \{\infty\}$. The set \mathbb{RP}^1 can be depicted as a circle. In our case, it is the unit circle in dark blue.



Instead of using the ∞ symbol, it is better to coordinatise its elements using homogeneous coordinates: The homogeneous coordinate $[x : y]$ (where $x \in \mathbb{R}, y \in \mathbb{R}$, and at least one of x or y is non-zero) represents the element $\frac{x}{y}$ of \mathbb{RP}^1 . There is a canonical projection map $\pi : \mathbb{R}^2 \rightarrow \mathbb{RP}^1, (x, y)^T \mapsto [x : y]$.

Every 2×2 real matrix M canonically acts on \mathbb{RP}^1 by $M.[x : y] = \pi(M(x, y)^T)$. Two matrices M and K admit the same canonical action on \mathbb{RP}^1 iff $M = \lambda K$ for λ some non-zero scalar.

A *hyperbolic line* is a cycle orthogonal to the unit circle, i.e. it meets the unit circle at a right angle. A *hyperbolic spear* is an *oriented* hyperbolic line. In particular, a hyperbolic spear is always its own orientation-reversed inversion. A given hyperbolic spear can be denoted by the ordered pair (p, q) where both p and q are in \mathbb{RP}^1 , and are the endpoints of the hyperbolic spear. Note that the term *hyperbolic* here might appear confusing given that there is no hyperbola, but this instead a reference to hyperbolic geometry, which we will not dwell upon.¹

Given a non-singular 2×2 real matrix M , we can consider the set of hyperbolic spears which represents its graph $\Gamma(M) := \{(p, M.p) : p \in \mathbb{RP}^1\}$. We then attempt to somehow summarise $\Gamma(M)$ using a single geometric figure.

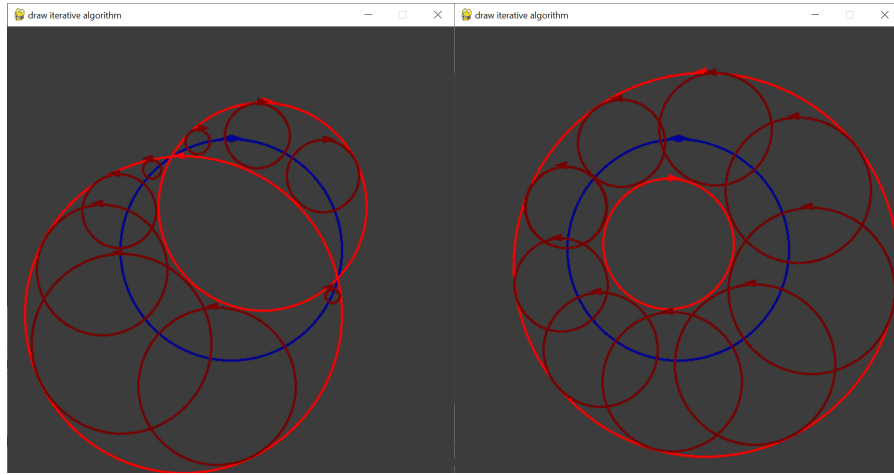
¹These are indeed the lines of hyperbolic geometry, as depicted in the Poincare disk model of hyperbolic geometry. The term “spear” usually refers to oriented lines in geometries in which the term “line” can be given a sensible meaning.

3.3 The non-negative determinant case

We intend to show that any non-zero matrix with non-negative determinant can be depicted as an oriented cycle and its orientation-reversed inversion. This includes all non-zero singular matrices.

Given an invertible matrix M with non-negative determinant, there is a unique pair of oriented cycles $\{C, \text{ORI}(C)\}$ such that each hyperbolic spear in $\Gamma(M)$ is orientedly tangent to both C and $\text{ORI}(C)$. We will verify this claim in the appendix using Lie Sphere Geometry.

We have an example of this below, where the elements of $\Gamma(M)$ are in dark red, and both C and $\text{ORI}(C)$ are in bright red:

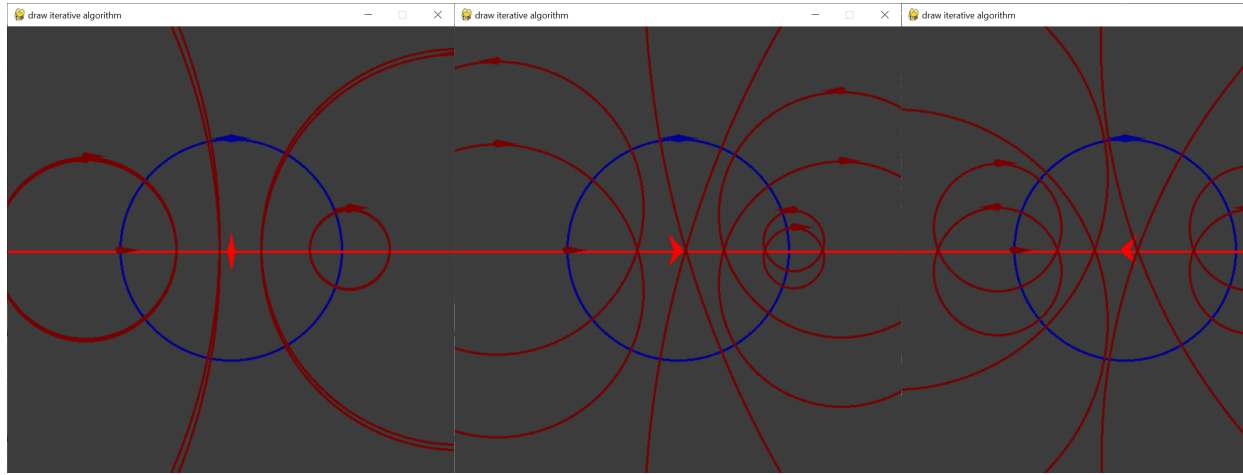


We may also pass to the limit where M is singular (but $M \neq \mathbf{0}$). The claim that there is a unique $\{C, \text{ORI}(C)\}$ corresponding to M still holds, as we will verify in the appendix.

3.4 The non-positive determinant case

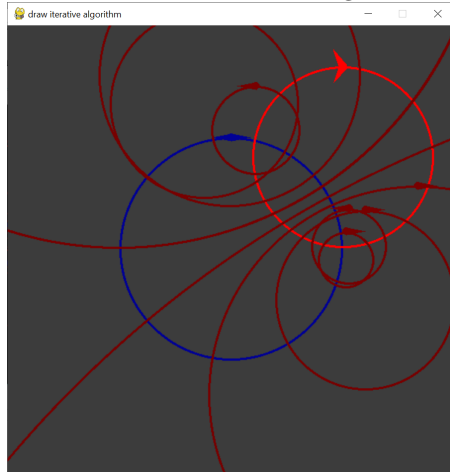
Consider a negative determinant matrix M . Essentially, its representation is a *continuously-oriented hyperbolic line* where the orientation is in the closed interval $[-1, +1]$ instead of in the set $\{-1, +1\}$.

To understand why: Consider the special case where M is diagonal.



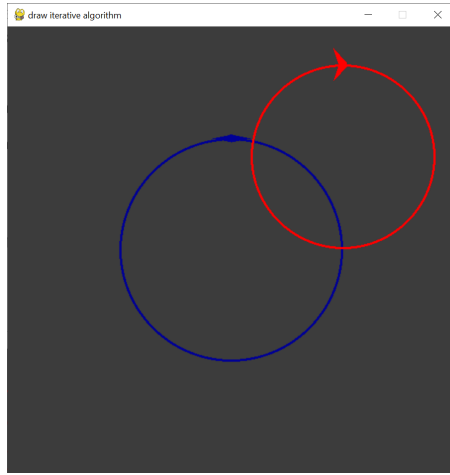
In dark red, we see $\Gamma(M)$. We see that all hyperbolic spears in $\Gamma(M)$ meet the hyperbolic line in bright red at two set angles. The two set angles are depicted by the *two* bright red arrow heads. We say that the orientation of the bright red line, which represents our matrix, is $\theta \in [-1, 1]$, if the angles of approach are $\pm \frac{\pi}{2}(1 + \theta)$. These are thus two different values, depicted using two arrow heads. In the event that $\theta \in \{-1, 1\}$, the two angles of approach will become the same, and so the bright red arrow heads will point in the same direction as each other. In that same event, the matrix M will be singular, and the visualisation will look identical to the non-negative determinant case.

The case where M is not diagonal looks as follows:



The only difference is that the bright red circle (which is the hyperbolic line depicting M) is no longer a straight line.

Since the dark red hyperbolic spears are merely scaffolding, we may remove them to get:



3.5 Visualising the naive QR algorithm for all non-negative determinant 2×2 real matrices

The QR algorithm is complicated enough to benefit from this visualisation. Here are some visualisations of the QR algorithm. The input matrix is given in red. The first iteration is in light blue. Subsequent iterations get lighter and lighter, until they're white. The user is expected to control one of the red circles by making it:

- Translate left, right, up, or down
- Shrink or expand
- Reverse in orientation

This determines the movement of the other red circle as well, which may then become a straight line. In this way, the user can traverse all possible input 2×2 real matrices with non-negative determinants.

Consider the red oriented cycles in each case:

- In case 1, we see that the dark blue circle meets the red cycle at two distinct points. The two points where the dark blue and red circles meet correspond to the *real eigenvectors*. Since in the two-circle case, we have $\det(M) \geq 0$, the eigenvalues of M have the same sign. Therefore, M is *diagonalisable with real eigenvalues of the same sign*.
- In case 2, we see that the the dark blue circle meets the red cycle at only one point. This one point is the sole real eigenvector of M . Therefore M is *non-diagonalisable, and its sole eigenvalue is real*.

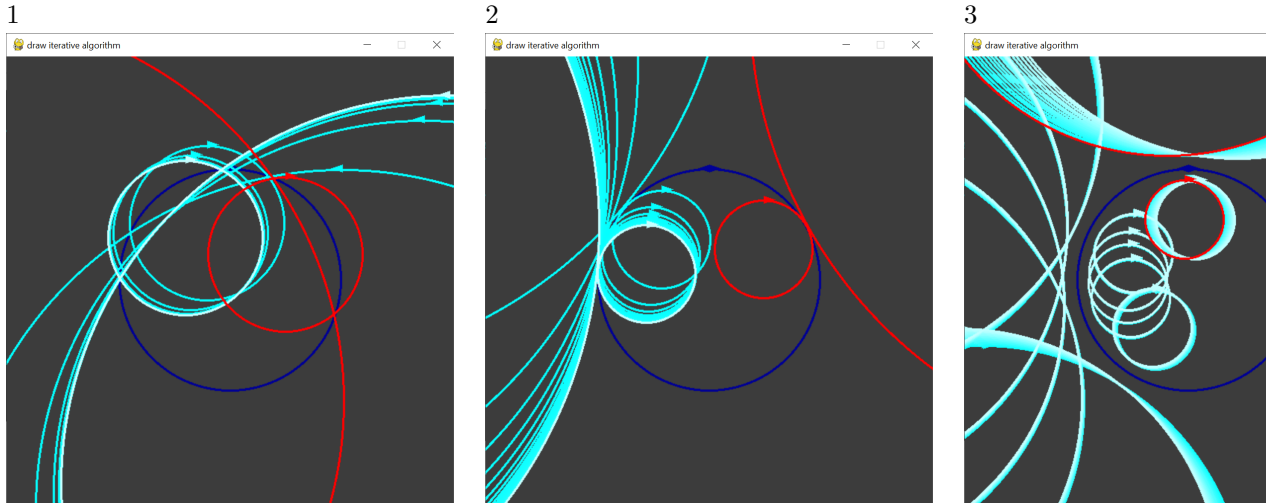


Table 1:

- In case 3, we see that the red cycle does not meet the dark blue circle. This means that M has no real eigenvectors. But it must have *some* eigenvector. This eigenvector is complex, and has a complex eigenvalue λ . Since $\bar{\lambda}$ is also an eigenvalue, we have that M is *diagonalisable with complex eigenvalues*.

These are 3 of the 4 possible Jordan Normal Forms of a 2×2 real matrix. The remaining case has the eigenvalues of M be real and with opposite signs, which we will investigate later.

Observe that each light-blue circle is obtained from the red circle by a rotation around the point in the plane $(0,0)$. This means that each iteration is orthogonally similar to the preceding iterations. This is easily explained by the definition of the QR algorithm.

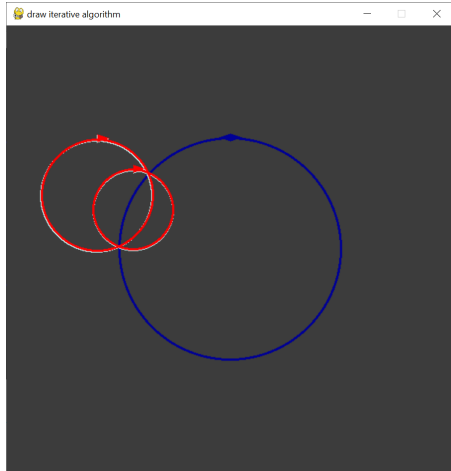
Observe the white circle(s): Clearly, in the first two cases, the algorithm converges, and in the third, it doesn't. But notice that – assuming convergence – the white circle passes through the point $(-1,0)$. A circle passing through $(-1,0)$ corresponds to an upper triangular matrix. The QR algorithm, when it converges, converges to an upper triangular matrix. The *very objective* of the QR algorithm is to successively reduce the angle between a cycle and the point $(-1,0)$.

Case 2 (the non-diagonalisable case) converges more slowly than case 1, but still converges. There is a transition from cases 1, to 2, to 3, where convergence gets slower until it stops happening.

We now explore behaviour near limits:

Case 5 is obtained from case 4 by an orientation reversal, which is the same thing as taking the matrix inverse. Case 4 is an attractive fixed point; small perturbations of it get mapped closer to the fixed point. Case 5 is a repuls-

4



5

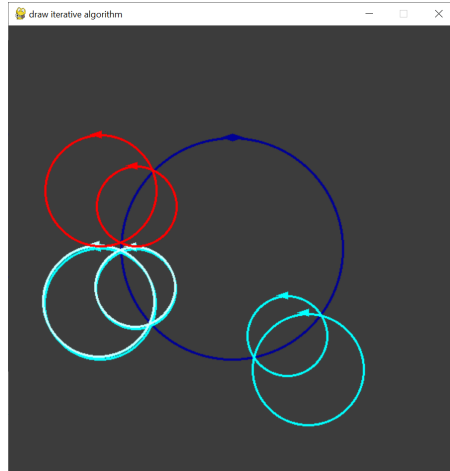


Table 2:

ive fixed point; small perturbations are mapped away from the fixed point. We see that the matrix inverse of an attractive fixed point is a repulsive fixed point.

Without explaining too much about this point (see [4, 1]: The existence of non-attractive fixed points is a consequence of the fact that an iteration of $(QR = M) \mapsto RQ$ is continuous in M . It is a topological fact as opposed to a quantitative fact. In order for a variant of QR to be practical, it must iterate a *discontinuous* map. Observe that Wilkinson shifts, for instance, introduce the necessary discontinuity.

Near the identity matrix, we see case 6:

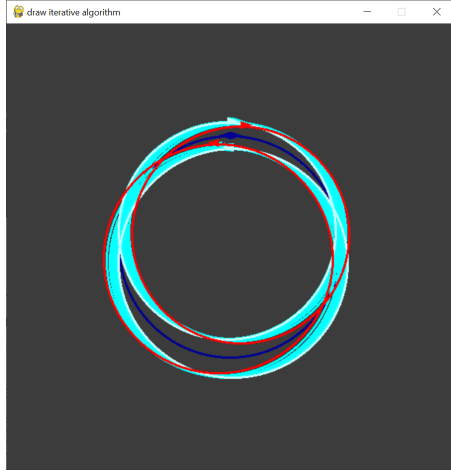
Case 6 has the two red cycles be very close to the dark blue circle (barely visible). This means they are close to the identity matrix. In this case, the algorithm converges very slowly, which can be seen from the large amounts of light blue. This behaviour happens because near an eigenvalue clash, the eigenspaces are unstable. For such a matrix, while we can estimate its eigenvalues accurately using the Gershgorin circle theorem, it is impossible to accurately determine its eigenvectors.

The complete opposite of case 6 is case 7. In this case, the two red cycles $\{C, \text{ORI}(C)\}$ are almost the same as each other. They are also nearly orthogonal to the dark blue circle, making them approximately hyperbolic spears. We see that *this is the case when M is nearly singular*. Convergence happens very quickly here.

Case 6 happens when $\frac{\lambda_1}{\lambda_2} \approx 1$, and its behaviour is thanks to fundamental computability considerations (finding eigenvectors for a matrix whose eigenvalues have unknown algebraic multiplicities is impossible), and case 7 happens when $\frac{\lambda_1}{\lambda_2} \approx 0$, and its behaviour is the opposite to case 6.

The objective of *shifting* an $n \times n$ matrix is to heuristically find a constant λ

6



7

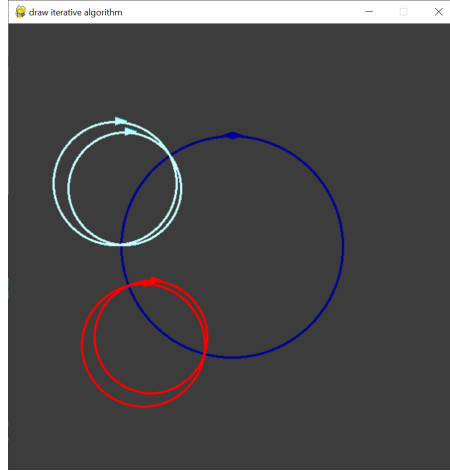


Table 3:

such that $M - \lambda I$ is approximately singular. This speeds up convergence. This is motivated by moving away from case 6 to case 7.

In the complex eigenvalue case, the algorithm displays near periodicity, except when M is near to an orthogonal matrix:

If the eigenvalues are $re^{\pm i2\pi m/n}$ for m/n in simplest form, then the periodicity of the iterates is n . If the eigenvalues are instead $re^{\pm i2\pi x}$ for x irrational, then the approximate periodicity is given by the rational approximations of x .

Case 9 involves a near-orthogonal matrix. This is nearly a fixed point.

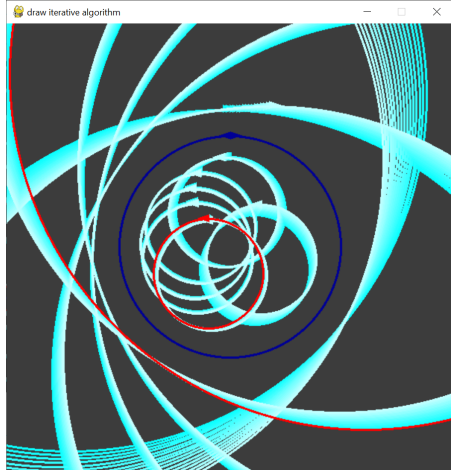
3.6 The naive QR algorithm in the negative determinant case

The user can rotate one of the arrow heads, and in so doing, the other arrow head. The user can specify the pair of points where the hyperbolic line representing the matrix meets the unit circle.

Note: In the negative determinant case, we post-multiply Q and pre-multiply R by $\begin{pmatrix} -1 & 0 \\ 0 & 1 \end{pmatrix}$ in order to

Below, we see some negative determinant cases. In these cases, the algorithm converges to one limit point when $\text{trace}(M) < 0$ (case 10), and a different one when $\text{trace}(M) > 0$ (case 12). When $\text{trace}(M) = 0$ (case 11), the algorithm oscillates between two points, both different from the limit points in the other cases; one of the limit points is the starting one; therefore, for small values of $\text{trace}(M)$, convergence is slow.

8



9

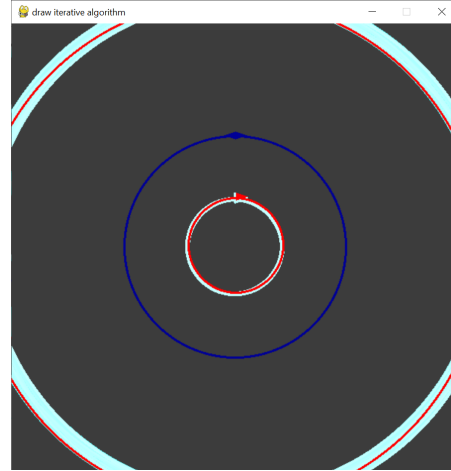


Table 4:

4 How v2 works (Lie Sphere Geometry)

4.1 Lie Sphere Geometry vs Euclidean vs Moebius

Here, we will introduce Lie Sphere Geometry [2], and use it to verify the above claims. It should be possible to reproduce the visualisations using this.

Lie Sphere Geometry (which we will abbreviate to LSG) is a generalisation of Moebius geometry, which is in turn a generalisation of Euclidean geometry.

4.2 Euclidean geometry

Euclidean geometry is the study of objects called *cycles*, which are either points, non-point circles, or lines. There is a group which acts on these called the Euclidean group, which is denoted $E(n)$ in dimension n . It is generated by the Euclidean reflections.

4.3 Moebius geometry

We turn to Moebius geometry. Synthetically (that is, without reference to coordinates) Moebius geometry is the study of the same cycles as in Euclidean geometry, except with an additional point at infinity. Euclidean motions generalise so as to fix the point at infinity. The real difference lies in the group, which consists of all conformal transformations, i.e. those which leave angles between cycles the same.

To perform Moebius Geometry analytically, it is helpful to provide coordinate systems. The points can be given homogeneous coordinates $[z : w]$, where

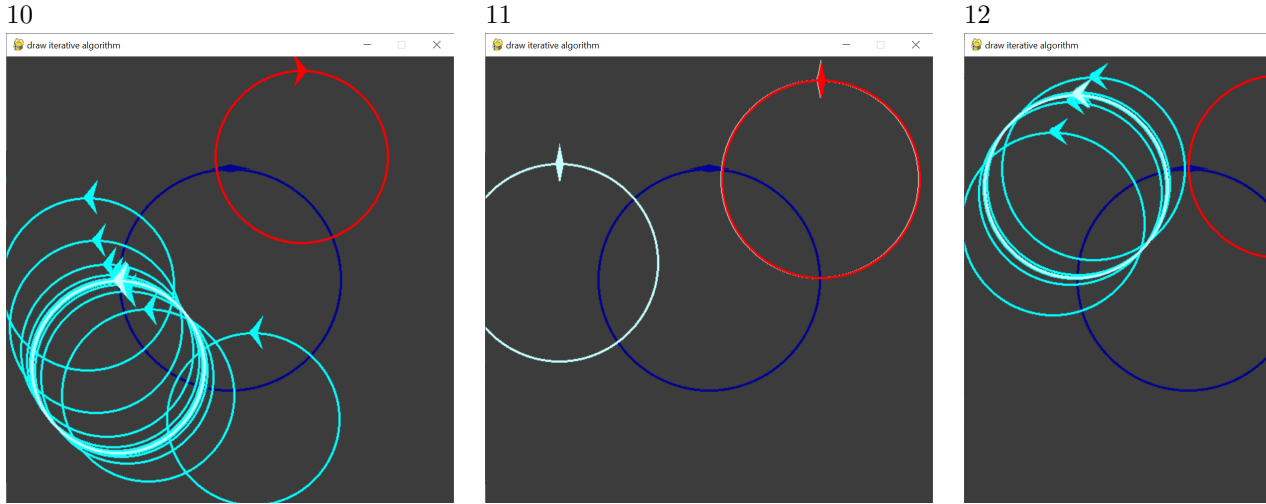


Table 5:

z and w are both complex numbers. Thus, the points are those of the projective line over the complex numbers, \mathbb{CP}^1 . Clearly, the point with homogeneous coordinate $[z : w]$ can be represented by the vector $(z, w)^T$.

The Moebius transformations form a group isomorphic to $\text{PGL}_2(\mathbb{C})$. This group consists of the invertible 2×2 complex matrices, modulo non-zero scalar factor.

The cycles in Moebius geometry can be coordinatised using *indefinite* 2×2 *Hermitian matrices*, modulo real scalar factor. A point p lies on cycle C iff $p^* C p = 0$, where p^* denotes the conjugate-transpose of p .

4.4 Lie Sphere Geometry

We now describe LSG. In LSG, the space consists of *oriented cycles*. These are either unoriented points, oriented non-point circles, or oriented lines. The transformation group consists of all those bijective maps which preserve oriented tangency. The transformation contains all the Moebius transformations and more; the non-Moebius transformations are not relevant to our discussion.

The space of oriented cycles can be coordinatised using some of the points of \mathbb{RP}^4 . Not every point in \mathbb{RP}^4 represents an oriented cycle. Rather, we define the *Lie quadric* \mathbb{L} , whose points are in 1-to-1 correspondence with oriented cycles in the plane, by $-x_1^2 - x_2^2 + x_3^2 + x_4 x_5 = 0$. Additionally, we define a method for checking whether the oriented cycles represented by two points p and q of \mathbb{L} are orientedly tangent. The method is to use the bilinear form B corresponding to the quadratic form which defines the Lie quadric \mathbb{L} , and check whether $B(p, q) = 0$. We prefer the notation $p \cdot q$ to $B(p, q)$. The transformation group is thus isomorphic to the projective linear group $\text{PO}_{2,3}(\mathbb{R})$.

The precise correspondence between points on \mathbb{L} and oriented cycles is as follows: A point $p \in \mathbb{L}$ either has:

- i. $p = [x_1 : x_2 : x_3 : x_4 : 1]$,
- ii. or $p = [x_1 : x_2 : 1 : x_4 : 0]$,
- iii. or $p = [0 : 0 : 0 : 1 : 0]$,

and these correspond respectively to:

- i. An oriented circle with centre point (x_1, x_2) , radius $|x_3|$, and orientation *inside the disk* if $\text{sign}(x_3) = -1$, or *outside the disk* if $\text{sign}(x_3) = 1$.
- ii. The oriented line given by the half-plane $x_1x + x_2y - 2x_4 \geq 0$.
- iii. The point at infinity.

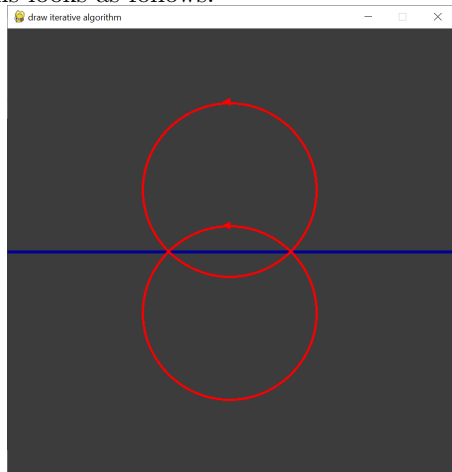
Using this correspondence, one can then check that indeed $p \cdot q = 0$ iff p and q are orientedly tangent.

4.5 Applying Moebius transformations to oriented cycles

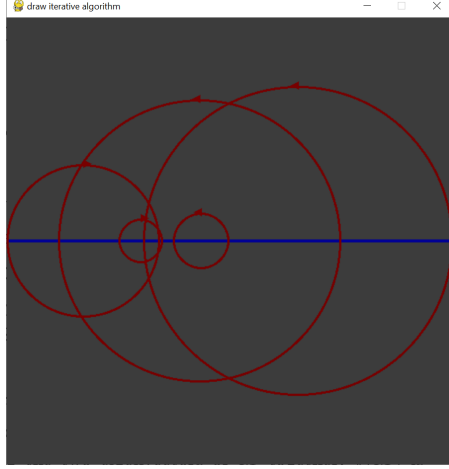
An oriented cycle $C = [-b : -c : * : d : a]$ corresponds to the unoriented cycle whose Hermitian matrix representation is $H = \begin{pmatrix} a & -b + ic \\ -b - ic & d \end{pmatrix}$. The term hidden by $*$ is one of $\pm\sqrt{-\det(H)}$. This correspondence enables one to evaluate Moebius transformations on oriented cycles.

4.6 Matrix as a bundle of hyperbolic spears

It is easier initially to represent the projective real line as the x -axis rather than as the unit circle. In this case, a nonnegative-determinant 2×2 real matrix is depicted as a pair $\{C, \text{RI}(C)\}$, where C is any oriented cycle, and $\text{RI}(C)$ denotes the result of reflecting C through the x -axis and then reversing its orientation. This looks as follows:



This is justified as follows: Every 2×2 real matrix M acts on the projective real line in a canonical way. We can represent the projective real line as the x -axis within the ambient space \mathbb{RP}^2 . We define a *hyperbolic spear* (in this context) to be an oriented cycle orthogonal to the x -axis. From any matrix M , we may produce the bundle $\Gamma(M)$ of hyperbolic spears connecting each point p on the x -axis to Mp . Depicting this for five values of p may look like:



The dark red circles are the elements of $\Gamma(M)$.

The hyperbolic spear connecting $p = [x : y]$ to Mp where $M = \begin{pmatrix} a & b \\ c & d \end{pmatrix}$ is given by $[-x(cx + dy) - y(ax + by) : 0 : x(cx + dy) - y(ax + by) : -2x(ax + by) : -2y(cx + dy)]$.

We may reduce $\Gamma(M)$ to a simple figure in each case:

In the positive determinant case: Given matrix $M = \begin{pmatrix} a & b \\ c & d \end{pmatrix}$, all the elements in $\Gamma(M)$ can be shown to be orientedly tangent to $\{C, \text{RI}(C)\}$ where $C = [a - d : 2\sqrt{ad - bc} : a + d : -2b : 2c]$ and $\text{RI}(C) = [a - d : -2\sqrt{ad - bc} : a + d : -2b : 2c]$. We see that this naturally extends to the zero determinant case. We see also that this formula *does not* work in the negative determinant case.

In the negative determinant case: Given a matrix $M = \begin{pmatrix} a & b \\ c & d \end{pmatrix}$ with $\det(M) < 0$, all the elements of $\Gamma(M)$ can be shown to meet some hyperbolic line $L(M)$ at angles $\pm \frac{\pi}{2}(1 + \theta(M))$. The $L(M)$ is the unique hyperbolic line connecting the two eigenvectors of M together. $\theta(M)$ is $-1 + \frac{2}{\pi} \arcsin((\lambda_1 + \lambda_2)/(\lambda_1 - \lambda_2))$. These claims can be verified by proving them in the case where M is diagonal – and $L(M)$ is thus the y -axis – and then generalising to non-diagonal $M = PDP^{-1}$ (with $\det(D) < 0$) by treating P as a Moebius transformation.

Finally, we apply a Moebius transform $z \mapsto \frac{1-iz}{1+iz}$ to send the x -axis to the unit circle. This produces the visualisation we've been using elsewhere in this paper.

5 Prospects for a generalisation to 3×3 matrices

5.1 Brief introduction

A possible criticism is that the above discussion is limited to 2×2 real matrices, where the QR algorithm is not strictly speaking used. In spite of that, it is useful to convey intuitively how the naive, uncomplicated algorithm behaves on the simplest inputs. The behaviour is complicated enough that a visualisation ought to have value. Here, we suggest an extension to the 3×3 case.

Some aspects of v2 can formally be generalised to 3×3 real matrices. Once again, one tries to take an *envelope* of some oriented figures. The problem is that the figures are now slightly more complicated, and the envelope – like already encountered in the 2×2 case – might not exist. In the 2×2 case, we know how to deal with this problem: If a matrix has negative determinant, then we need to use a certain *generalisation* of an envelope that we described above. What the appropriate generalisation might be in the 3×3 case is not clear.

5.2 Details

Let M be a 3×3 real matrix. M acts in a natural way on the projective plane \mathbb{RP}^2 . While an element of \mathbb{RP}^2 may be a point, it is actually more convenient to choose it to be a *projective line*, thanks to projective duality. Embed \mathbb{RP}^2 as a plane Π within the ambient projective space \mathbb{RP}^3 . Given a line l on Π , M maps it to $M(l)$. Connect l to $M(l)$ using an *oriented right circular cone*. This oriented figure will necessarily exist and be unique, even when $M(l)$ is the unique line at infinity on Π . Finally, one must (if possible) take the envelope of all of these oriented right circular cones, each one corresponding to a different line l . The resulting envelope may or may not exist, but some sort of generalisation of an envelope may be applicable (see the discussion above).

Acknowledgements I would like to thank Jan Techter, Gregory Gutin and Abbas Edalat for some helpful discussions.

References

- [1] Jess Banks, Jorge Garza-Vargas, and Nikhil Srivastava. Global convergence of hessenberg shifted qr i: dynamics. 2021.
- [2] Walter Benz. *Sphere Geometries of Möbius and Lie*, pages 93–174. Springer Basel, Basel, 2012.
- [3] Hendrik Jan Buurema. *A geometric proof of convergence for the QR method*. Rijksuniversiteit te Groningen, Groningen, 1970. Doctoral dissertation, University of Groningen.

- [4] Ricardo S. Leite, Nicolau C. Saldanha, and Carlos Tomei. Dynamics of the symmetric eigenvalue problem with shift strategies. *Int. Math. Res. Not. IMRN*, (19):4382–4412, 2013.
- [5] David S. Watkins. The QR algorithm revisited. *SIAM Rev.*, 50(1):133–145, 2008.